# Method for Estimating the Sonic-Boom Characteristics of Lifting Canard-Wing Aircraft Concepts

*Robert J. Mack*
*Langley Research Center, Hampton, Virginia*

Since its founding, NASA has been dedicated to the advancement of aeronautics and space science. The NASA Scientific and Technical Information (STI) Program Office plays a key part in helping NASA maintain this important role.

The NASA STI Program Office is operated by Langley Research Center, the lead center for NASA's scientific and technical information. The NASA STI Program Office provides access to the NASA STI Database, the largest collection of aeronautical and space science STI in the world. The Program Office is also NASA's institutional mechanism for disseminating the results of its research and development activities. These results are published by NASA in the NASA STI Report Series, which includes the following report types:

- TECHNICAL PUBLICATION. Reports of completed research or a major significant phase of research that present the results of NASA programs and include extensive data or theoretical analysis. Includes compilations of significant scientific and technical data and information deemed to be of continuing reference value. NASA counterpart of peer-reviewed formal professional papers, but having less stringent limitations on manuscript length and extent of graphic presentations.

- TECHNICAL MEMORANDUM. Scientific and technical findings that are preliminary or of specialized interest, e.g., quick release reports, working papers, and bibliographies that contain minimal annotation. Does not contain extensive analysis.

- CONTRACTOR REPORT. Scientific and technical findings by NASA-sponsored contractors and grantees.

- CONFERENCE PUBLICATION. Collected papers from scientific and technical conferences, symposia, seminars, or other meetings sponsored or co-sponsored by NASA.

- SPECIAL PUBLICATION. Scientific, technical, or historical information from NASA programs, projects, and missions, often concerned with subjects having substantial public interest.

- TECHNICAL TRANSLATION. English-language translations of foreign scientific and technical material pertinent to NASA's mission.

Specialized services that complement the STI Program Office's diverse offerings include creating custom thesauri, building customized databases, organizing and publishing research results ... even providing videos.

For more information about the NASA STI Program Office, see the following:

- Access the NASA STI Program Home Page at *http://www.sti.nasa.gov*

- E-mail your question via the Internet to help@sti.nasa.gov

- Fax your question to the NASA STI Help Desk at (301) 621-0134

- Phone the NASA STI Help Desk at (301) 621-0390

- Write to:
  NASA STI Help Desk
  NASA Center for AeroSpace Information
  7121 Standard Drive
  Hanover, MD 21076-1320

# Method for Estimating the Sonic-Boom Characteristics of Lifting Canard-Wing Aircraft Concepts

*Robert J. Mack*
*Langley Research Center, Hampton, Virginia*

December 2005

Available from:

**Summary**

A method for estimating the sonic-boom overpressures from a conceptual aircraft where the lift is carried by both a canard and a wing during supersonic cruise is presented and discussed. Computer codes used for the prediction of the aerodynamic performance of the wing, the canard-wing interference, the nacelle-wing interference, and the sonic-boom overpressures are identified and discussed as the procedures in the method are discussed. A canard-wing supersonic-cruise concept was used as an example to demonstrate the application of the method.

**Introduction**

The most common design for a supersonic-cruise aircraft is a wing/body/nacelle/fin configuration with sufficient wing and fuselage volume to hold passengers, cargo, and fuel for the performance of a specified mission. Wing area is usually sized to meet takeoff and efficient cruise constraints. Engines capable of mission performance are usually located along the trailing edge of the wing for aerodynamic and structural efficiency. A fin (or fins) of sufficient area to meet flight and engine-out control criteria is usually mounted on the aft fuselage for maximum effect.

Toward the end of the preliminary concept design phase, the designer often found there was insufficient elevator or elevon power available to meet takeoff rotation, landing, and low-speed handling requirements. Then, an auxiliary surface, such as a canard or a horizontal tail, would be considered to meet these mission requirements. When the canard or the horizontal-tail surface was used only during the low-speed segments of the mission, and did not carry lift during the supersonic-cruise segment of the mission, the existing methods for predicting sonic-boom characteristics would suffice, since these auxiliary surfaces generated only volume disturbances. However, if part of the aircraft's weight was carried by a canard during the cruise segment of the mission, then its lift and the effect of its downwash on the wing needed to be included in the analytical methods for predicting the aircraft's sonic boom pressure signature on the ground. Similarly, a horizontal tail carrying lift during cruise, might be in the downwash from the wing. Then, its lift contribution needed to be modified by this downwash field. So, if the configuration had a lifting canard that influenced the wing lift, or a lifting horizontal tail influenced by the lifting wing, their volume and lift contributions to the aircraft's sonic-boom disturbances required special treatment.

Since a lifting canard and a horizontal tail required special treatment in a sonic-boom analysis, their total contributions needed to be outlined and explained. However, the scope of this report focused only on the lifting-canard / wing configuration. A method for estimating the sonic-boom overpressures from a lifting-canard/wing supersonic-cruise conceptual aircraft was outlined and discussed. Then, the method was demonstrated by the prediction of the sonic- boom ground overpressures from a hypothetical lifting-canard / wing concept. Since sonic-boom overpressures are the main consideration in this sample exercise, it was assumed that the canard-wing concept was capable of fulfilling all specified mission requirements. It should be noted, however, that the techniques discussed in this paper could also be applied to the horizontal tail's sonic-boom contributions if it was seriously affected by the wing's downwash field.

## Nomenclature

| | |
|---|---|
| $A_E$ | equivalent area, $ft^2$ |
| $A_{E,CW}$ | equivalent area due to canard-wing interference lift, $ft^2$ |
| $A_{E,L,C}$ | equivalent area due to the lift of the canard surface, $ft^2$ |
| $A_{E,L,W}$ | equivalent area due to the lift of the wing, $ft^2$ |
| $A_{E,L,INT}$ | equivalent area due to the nacelle-wing interference lift, $ft^2$ |
| $A_{E,VOL,NAC}$ | equivalent area due to the volume of the nacelle, $ft^2$ |
| $A_{E,VOL,WFCF}$ | equivalent area due to the volume of the wing, fuselage, canard, and fin(s), $ft^2$ |
| $C_{L,CAN}$ | lift coefficient of the deflected canard |
| $C_{L,CAN,O}$ | lift coefficient of the canard at zero deflection angle |
| $C_{L,CAN/W}$ | lift coefficient induced by the canard on the wing |
| $C_{L,CAN/W,O}$ | lift coefficient induced on the wing by the canard at zero deflection angle |
| $C_{L,NAC}$ | lift coefficient due to nacelle-wing interference |
| $C_{L,W}$ | lift coefficient of the isolated wing |
| $C_{L,WING}$ | lift coefficient of the wing in the presence of the canard |
| $C_{L,W,O}$ | lift coefficient of the isolated wing at zero angle of attack |
| $C_{L,TOT}$ | lift coefficient of the aircraft |
| $F(y)$ | Whitham F-function of parameter y, $ft^{1/2}$ |
| $l$ | length of aircraft, ft |
| $l_e$ | effective length of the aircraft, ft |
| $h$ | beginning-cruise altitude, ft |
| $M$ | cruise Mach number |
| $p$ | ambient pressure, psf |
| $\Delta p$ | increment in pressure due to the aircraft, psf |
| $q$ | flight dynamic pressure, psf |
| $S_{REF}$ | reference wing area, $ft^2$ |
| $W_{CR}$ | aircraft weight at start of cruise, lb |
| $x$ | distance along longitudinal axis, ft |
| $x_e$ | effective distance along the longitudinal axis, ft |

| y | distance along the spanwise direction or F-function parameter, ft |
|---|---|
| $\alpha$ | angle of attack at cruise, deg |
| $\Delta$ | increment |
| $\delta$ | canard surface deflection angle, deg |
| $\Lambda$ | leading-edge sweep angle, deg |
| $\left(\dfrac{\Delta C_L}{\Delta \alpha}\right)$ | wing lift slope at zero angle of attack, per deg |
| $\left(\dfrac{\Delta C_L}{\Delta \delta}\right)$ | wing lift slope due to canard deflection, per deg |

## Lift Slope Subscripts

| CAN | canard |
|---|---|
| CW | canard-wing interference |
| INT | nacelle-wing interference |
| L | lift |
| O | zero angle of attack or zero deflection angle |
| TOT | total |
| VOL | volume |
| W | wing |

A dot or a double dot above a symbol signifies a first or a second derivative with respect to the independent variable.

# Method

The sonic-boom characteristics of a simple wing-fuselage aircraft can be estimated with the methods presented in references 1 and 2. They are reviewed to provide a background for the procedure reported in this paper that included the effects of a lifting canard. Modifications to the sonic-boom analysis methods that treat ducted nacelle volume, nacelle-wing interference lift, canard lift, as well as the downwash field contributions from the canard lifting surface are also presented and discussed.

Five steps are required to predict the ground pressure signatures. First, equivalent areas due to volume are obtained, references 3 and 4, from the concept's components that have smooth and continuous normal-area distributions. Wing, fuselage, fin, and perhaps canards and/or horizontal tails usually met this constraint. These smooth-and-continuous surface contour equivalent areas are used to calculate the first Whitham F-function.

Second, equivalent areas due to volume are obtained from the components with surface discontinuities, and used to obtain a second F-function or a second set of F-functions. Engine nacelles, which require this treatment, are usually ducted bodies of revolution. Normal areas, instead of "Mach-sliced" (area-ruled) areas, can be used with the Whitham theory method described in reference 5 to obtain the required F-function(s).

Third, the aircraft's wing and canard geometry are used to obtain aerodynamic lift, drag, and pitching moment characteristics as well as "Mach-sliced" lift-induced equivalent areas, from the methods described in reference 6, if these equivalent area distributions are smooth and continuous. The method of reference 7 was used to calculate the canard-wing interference lift equivalent areas when they are smooth and continuous. These equivalent areas provided the input data for the third set of F-function(s).

Fourth, the nacelle-wing interference lift equivalent areas from each pair of nacelles are calculated with the method of reference 5. If a nacelle is mounted on the concept's centerline, then its nacelle-wing interference lift equivalent areas are calculated separately. These equivalent areas are used to obtain the corresponding F-function(s).

In the fifth step, the F-functions obtained in the previous four steps are summed to obtain an aircraft or concept F-function. This summed F-function is used as the input to the computer code described in reference 8 so that the desired ground-level pressure signature can be predicted.

## Determination Of Lift And Lift Distributions

A concept's geometry, described in the format of references 3 and 4, provided the starting point in the sonic-boom analysis and prediction procedure. The configuration's description was used to calculate the nacelle-wing interference lift, drag, and pitching-moment, the wing lift, and the canard lift. The summed lift, drag, pitching moment, skin friction, and roughness data were inputs for the estimation of supersonic-cruise mission performance during cruise. Cruise Mach number, beginning-cruise weight, and beginning-cruise altitude were combined with the aircraft's calculated volume and lift equivalent areas the sonic-boom pressure signature on the ground could be predicted.

### Nacelle-Wing Interference Lift

The incremental lift generated by the nacelles under the wing's lower surface (or above the wing's upper surface) was estimated with the method of reference 5. It was calculated first because it was assumed to be almost constant through small changes in angle of attack. After the nacelle-wing interference lift was calculated, the lift contributions of the wing, the canard, and the canard-wing interference lift were calculated. If the angle-of-attack change significantly affected the nacelle-wing interference lift, then all the lift component calculations needed to be repeated and iterated to obtain the total lift that depended on the cruise Mach number, the beginning-cruise weight, and the beginning-cruise altitude.

### Wing and Canard Lift

The wing behind a lifting canard would suffer some performance penalty due to its presence in the canard's downwash field. This penalty would be proportional to the canard's lift and span, and inversely proportional to the square of the distance between the canard and the wing panels.

First, the performance of the isolated wing and the isolated canard was calculated with the method of reference 6. Then, the canard downwash interference on the wing was obtained from canard and wing geometry using the method of reference 7. Although the method of reference 7 is a linear-theory code, it provided a first-order estimate of canard-wing interference effects for a preliminary concept design analysis. Higher-order codes could be used later should the configuration show promise as a viable low-boom and/or a mission-capable concept. Finally, the lift on both the wing and the canard along with the cruise angle of attack could be found, iteratively if necessary, from the following set of equations:

$$C_{L,TOT} = C_{L,WING} + C_{L,CAN} + C_{L,NAC} + C_{L,CAN/W} \tag{1}$$

$$C_{L,TOT} = W_{CR} / qS_{REF} \tag{2}$$

$$C_{L,CAN/W} = C_{L,CAN/W,O} + \left(\frac{\Delta C_L}{\Delta \delta}\right)_{CW} \delta \tag{3}$$

$$C_{L,W} = C_{L,W,O} + \left(\frac{\Delta C_L}{\Delta \alpha}\right)_W \alpha \tag{4}$$

$$C_{L,CAN} = C_{L,CAN,O} + \left(\frac{\Delta C_L}{\Delta \delta}\right)_{CAN} \delta \tag{5}$$

$$C_{L,WING} = C_{L,W} + C_{L,CAN/W} \tag{6}$$

Equations (1) to (6) showed a linear variation in wing, canard, or canard/wing interference lift, even though some of them were obtained from computer codes based on non-linear theory. This indicated that they were intended for use only for small angles of attack. Since the method was applicable to preliminary concept design and analysis, this limitation should not pose significant problems.

Usually, the variables $C_{L,CAN/W,O}$ and $C_{L,CAN,O}$ were zero because the canard surface is given a flat-plate camber, and is mounted at zero-lift attitude relative to the wing's reference plane. When the canard has an all-moving surface, and its control deflection is held constant, lift coefficient increments from equations (3) and (5) are fixed. Then, the angle of attack appears only from the wing contribution in equation (4). The situation is more complicated if the canard is fixed and the wing trailing edge control surfaces are moved for pitch control. As the aircraft is pitched up to attain cruise lift, the canard will generate lift unless the surface is negatively deflected to nullify this lift. Now, the angle of attack appears in equations (3), (4), and (5) because the canard deflection is the model attitude plus an initial deflection angle. In this paper, the canard will be assumed to be an all-moving pitch-control surface held at a constant deflection during the the cruise segment of the mission.

Rates of change in equations (3) and (5) were obtained from the outputs of the canard analysis code, reference 7, where only the outer control panel was deflected. The rate of change in equation (4) was obtained from the wing analysis code, reference 6, which also supplied isolated wing data, and isolated canard performance data for comparison with data from reference 7. These six equations were then used to obtain a first-order estimate of the cruise angle of attack, the wing lift, the canard lift, and the canard-wing interference lift coefficients.

## Equivalent Areas and F-Functions

Two sources provided the equivalent area contributions that were used to compute the conceptual aircraft's F-function. Aircraft and nacelle volume were the first source, and their effects were estimated with the sonic-boom theory of Whitham, reference 8. Wing lift, canard lift, and nacelle-wing interference lift were the second source, and their effects were estimated with Walkden's extension to Whitham theory, reference 9. All but two of these equivalent area distributions had first and second derivative smoothness and continuity, so they could be used directly to calculate F-functions. When the component geometry and equivalent area distribution lacked these required smoothness qualities, different techniques were employed to obtain the required Whitham F-functions and are discussed in the following sections.

### Aircraft Volume

With the method described in references 3 and 4, the aircraft volume was area-ruled to supply the first incremental contribution, $\Delta A_E$, to the total $A_E$:

$$\Delta A_E = A_{E,VOL,WFCF}$$

The nacelle contributions were computed separately because their equivalent areas had a non-zero radius and a non-zero first derivative of the area at the inlet lip. This contribution is discussed in the section on *Nacelle Volume*.

Since the wing, fuselage, canard, and fin components usually had first and second derivative continuity, the equivalent areas used to compute a volume-contribution F-function were inputs to the smooth-and-continuous version, reference 9

$$F(\tau) = \frac{1.0}{2.0\pi} \int_0^\tau \frac{\ddot{A}_E(t)dt}{\sqrt{\tau-t}} \tag{7}$$

subject to the same limitations mentioned in the following paragraph concerning lift.

### Wing and Canard Lift

The analysis methods given in reference 6 and 7 were used to obtain the equivalent area contributions from the wing lift, the canard lift, and the canard-wing interference lift. These increments, $\Delta A_E$, were:

$$\Delta A_E = A_{E,L,W} + A_{E,L,C} + A_{E,CW}$$

A Whitham F-function, like that given in equation (7), was calculated from these summed components and added to the F-function from the volume contributions. If there were sizeable lengths of supersonic leading edge, leading-edge sweep cranks where the leading-edge sweep changed dramatically, or leading-edge cranks where the leading-edge sweep parameter $\beta \cot\Lambda$ changed from subsonic to supersonic on the wing or canard, then the F-function would need to be corrected to account for these discontinuities.

### Nacelle Volume

Engine nacelle equivalent area increments, $\Delta A_E$, could be computed with the computer code presented and described, in references 3 and 4, with the input areas

$$\Delta A_E = A_{E,VOL,NAC}(t)$$

used in equation (7) to obtain an F-function. Corrections for the inlet lip area and area slope discontinuities, as well as other abrupt changes in radii, must be calculated separately and included in the F-function calculation.

However, if the nacelles could be described as bodies of revolution, an F-function could be computed from normal areas, $A_{E,VOL,NAC}(x)$, with the method described in references 5 or 9. Engine nacelles must be treated separately because they have normal areas that were non-zero at the nacelle lip, and begin with non-zero first derivatives. The Stieltjes integral form of the Whitham F-function given in reference 9 and used in reference 5 included this correction.

The nacelles usually occur in pairs; an inboard pair, and if the concept has four engines mounted over/under the wing, an outboard pair. So, the F-function magnitude was doubled for each nacelle pair, then added, at the appropriate effective length station, to the aircraft smooth-and-continuous volume and lift F-function. Both the inboard and the outboard nacelles were handled similarly, but if an engine nacelle was mounted on the fuselage center line, only a single Whitham F-function was required.

## Nacelle-Wing Interference Lift

The same special treatment mentioned previously for nacelle volume was given to the increment in nacelle-wing interference-lift equivalent areas, $\Delta A_E$:

$$\Delta A_E = A_{E,L,INT}$$

In this case, the interference-lift equivalent areas from nacelle pairs were used (unless there was a nacelle on the line of symmetry) to compute the F-function from equation (7) and the associated corrections. Both the inboard and the outboard nacelle pairs contributed two Whitham F-functions to the total aircraft F-function.

This method for calculating nacelle-wing interference lift was based on the assumption that the entire nacelle-wing interference zone was within the wing planform area. If the interference zone spilled across part of the wing tip, a small and usually negligible error was introduced. However, if the interference zone spilled over the leading edge, then the interference disturbances would be felt on both upper and lower surfaces. If the "spill-over" area was small, this method would have decreased accuracy, but could still be useful; if the "spill-over" area was relatively large, a different method would be required to obtain a reasonably accurate value.

## Pressure Signature Calculation

The final F-function containing the sum of all the contributions of the aircraft's volume and lift was used as input to the *ARAP* code, reference 10, to obtain a predicted pressure signature which had propagated from the aircraft at cruise altitude through a standard or a specified atmosphere to the ground. Contributions to this aircraft's F-function were from:

Volume: wing, fuselage, fin(s) (smooth-body F-function, usually)
 nacelles (discontinuous-body F-function)

Lift: wing (smooth-body F-function, usually)
 canard (smooth-body F-function, if it has a subsonic leading edge, or
 discontinuous F-function, if it had a supersonic leading edge)
 nacelle-wing interference (discontinuous-body F-function)

In the following *Application* section, the sonic-boom overpressures of a canard/wing/fuselage/fin/nacelle conceptual aircraft configuration are calculated and evaluated. The canard on this concept would be contributing some of the lift needed to support the weight during supersonic cruise. Each of the steps required to calculate these volume and lift contributions is described

## Application

A conceptual aircraft, the HSCT-14, was designed to explore the mission performance capabilities and the reduced sonic-boom possibilities of a conceptual canard-wing aircraft in which the canard, as well as the wing, carried lift on the aircraft. On other canard-wing configurations, the canard was set for zero lift during the supersonic cruise segment of the mission. It was used only to rotate the aircraft at takeoff, and to help control the aircraft in pitch during the low-speed segments of the mission.

The supersonic-cruise segment of the mission was to be flown at a cruise Mach number of 2.4, with the total mission range set at 5000 nautical miles. Aerodynamic performance characteristics of this concept, calculated for the mission analysis and for an evaluation of its sonic-boom characteristics, were obtained from a numerical description of the computer-generated three-view schematic of the HSCT-14 shown in figure 1. A description of the aircraft's dimensions, and the mission data used for performance and sonic-boom calculations is presented in Appendix A. Drawings of the wing and the canard planforms are presented in figures 2 and 3 respectively.

### Nacelle-Wing Interference Lift

The incremental lift coefficient generated by the engine nacelles mounted under the wing, $C_{L,NAC}$, was estimated with the method described in reference 5. For this configuration, the value computed with no wing area "blanketed" or "shielded" by the nacelle volume was

$$C_{L,NAC} = 0.00427$$

This nacelle-wing interference lift estimate would be refined later if the final nacelle location was changed. Then, the actual wing area affected by nacelle disturbances would be determined. It was used in this analysis because it maximized the nacelle-wing interference lift contribution to the concept's potential for generating flow-field disturbances, and provided the most conservative prediction of sonic-boom ground overpressures. For small angles of attack, this value of $C_{L,NAC}$ would be assumed constant. The remaining contributions to the lift: the wing lift; the canard lift; and the canard-wing interference lift; were now determined.

### Wing and Canard Lift

The canard lift distribution began about 15 feet behind the nose. Although the main panels of the wing were well aft of the canard, the central wing section, which began 63.0 feet aft of the nose, was entirely within the canard's downwash field. With so much area affected, the wing required an additional increment in angle of attack to generate it's contribution to the cruise lift. This, unfortunately, generated an incremental drag-due-to-lift penalty. Thus, one result of the conceptual aircraft's performance analysis would be to determine the net effect obtained by sacrificing increments of aerodynamic performance for possible sonic-boom reduction.

As mentioned previously, the three rates of change in equations (3), (4), and (5) were first-order

accurate only. Their values were obtained from the canard-wing analysis code, reference 6, and the wing analysis code, reference 5, which supplied isolated canard performance, isolated wing performance, and canard-wing interference lift data, respectively. These six equations were then used to obtain a first-order estimate of the cruise angle of attack, the wing-lift coefficient, the canard-lift coefficient, and the canard-wing interference lift coefficient.

Beginning-cruise conditions were:

$$M = 2.4$$

$$h = 56,400 \text{ ft}$$

$$W_{CR} = 693,000 \text{ lb}$$

These three conditions set the net lift coefficient, $C_{L,TOT}$, as:

$$C_{L,TOT} = 0.09139$$

Wing: The wing planform was given a "mild" camber and twist distribution. Some flat-plate lift would be required to obtain cruise lift. A slightly-rounded leading edge provided some leading-edge thrust benefits that compensated for not employing more camber and twist. The method reported in reference 6 was used to obtain:

$$C_{L,W,O} = 0.03136,$$

$$\left(\frac{\Delta C_L}{\Delta \alpha}\right)_W = 0.02735 \text{ / deg,}$$

Canard: The canard had a flat camber and was designed to generate zero lift at zero deflection. So, by definition:

$$C_{L,CAN,O} = 0.0,$$

$$C_{L,CAN/W,O} = 0.0,$$

The other canard data needed in the mission performance analysis and in the prediction of sonic-boom characteristics were calculated from the method reported in reference 7. Their values, accurate to first order, were:

$$\left(\frac{\Delta C_L}{\Delta \delta}\right)_{CW} = -0.00135 \text{ / deg,}$$

$$\left(\frac{\Delta C_L}{\Delta \delta}\right)_{CAN} = 0.000997 \text{ / deg.}$$

For comparison, the lift slope of the isolated canard in the free stream could be calculated with the method reported in reference 6. The value calculated by this second method was:

$$\left(\frac{\Delta C_L}{\Delta \alpha}\right)_{CAN} = 0.00150 \text{ / deg.}$$

This value was larger because the whole canard planform rather than just the control panels, were contributing to the lift. It was used as a check to assure the value calculated with the first method was not over-estimated.

The canard surface on the configuration was arbitrarily deflected 5 degrees, i.e.:

$$\delta = 5.0 \text{ deg}$$

This deflection resulted in a canard lift coefficient, $C_{L,CAN}$ , contribution of:

$$C_{L,CAN} = C_{L,CAN,O} + \left(\frac{\Delta C_L}{\Delta \delta}\right)_{CAN} \delta = 0.00499$$

that was about 5.5 percent of $C_{L,TOT}$. Thus, the canard started the distribution of lift well forward of the wing. However, its contribution to the total lift was small enough that it did not act as a tandem wing and usurp the role of the wing as the main source of lift.

Now, the lift coefficient of the isolated wing, $C_{L,W}$, can be calculated by substituting the preceding values into equations (1) to (6) to obtain the first-order estimate of:

$$C_{L,W} = C_{L,TOT} - C_{L,NAC} - \left(\frac{\Delta C_L}{\Delta \delta}\right)_{CW} \delta - \left(\frac{\Delta C_L}{\Delta \delta}\right)_{CAN} \delta = 0.08889$$

The lift coefficient of the wing in the presence of a lifting canard can be calculated from:

$$C_{L,WING} = C_{L,W} + C_{L,CAN,W} = 0.08214$$

With these lift calculations, the additional wing angle of attack required to compensate for the induced downwash from the lifting canard was calculated to be:

$$\alpha = (C_{L,W} - C_{L,WING}) / \left(\frac{\Delta C_L}{\Delta \alpha}\right)_W = 0.25 \text{ deg (approximately)}$$

This was the additional increment in angle of attack required by the wing/fuselage/nacelles/canard/fin configuration to maintain cruise with the canard deflection set at 5 degrees.

For comparison, the cruise angle of attack required for the isolated wing, or the wing with a non-lifting canard, to carry the cruise weight was, using equations (2) and (4), about 2.10 degrees. Addition of the nacelle-wing interference lift to the isolated wing lift reduced the required cruise angle of attack from 2.10 degrees to about 1.95 degrees. So the lift-carrying canard required a small wing angle-of-attack increment, 0.25 deg, to be added to that required to support the vehicle with wing lift and nacelle-wing interference lift only. Although small, it induced an incremental drag-due-to-lift penalty that, when added to the drag-due-to-lift of the canard, resulted in a decrement in cruise-range performance.

The mission range was specified as 5000 nmi., but for the sake of brevity, the calculation of range performance was not addressed or discussed in this report. As was mentioned at the beginning of this report, it was assumed that mission range, takeoff field length, engine out yaw control, gross takeoff weight, mission fuel capacity, etc. criteria could be met. Never the less, this drag due to lift increment due to the canard's lift contribution was mentioned because, due to the resulting reduction in calculated mission range performance, it would be a factor in the concept's preliminary design.

# Equivalent Areas and F-functions

## Aircraft Volume

The area-rule calculation capability of the wave drag code, references 3 and 4, provided the equivalent area distribution at cruise angle of attack, figure 4, of the wing, canard, fuselage, and fin, $A_{E,VOL,WFCF}$, for estimation of sonic-boom directly under the flight path. Although the canard had a section of supersonic leading edge, its equivalent area was included with those of the wing, fuselage, and fin because it was located at the aircraft nose and the appropriate F-function could be corrected. The nacelle volumes were handled separately because their volume equivalent area growth and nacelle-wing interference lift equivalent area growth had discontinuities due to a non-zero slope and a finite radius at the inlet lip. The treatment of these two effects is described in the following sections on *Nacelle Volume* and *Nacelle-Wing Interference Lift*.

## Wing and Canard Lift

Equivalent areas due to the lift of both the wing and the canard, $A_{E,L,W}$ and $A_{E,L,C}$ respectively (figures 5 and 6) were calculated with the method described in reference 6 using the values of the wing lift coefficient, $C_{L,WING}$, the canard lift coefficient, $C_{L,CAN}$, and the cruise angle of attack, $\alpha$. The method of reference 7 was used to obtain the equivalent area distribution due to canard-wing interference lift. These equivalent area contributions, figures 4 through 7, were summed in figure 8, and used to calculate the F-function shown in figure 9.

## Nacelle Volume

The F-function of each engine nacelle was calculated by computing the F-function from normal areas using the Stieltjes integral method of reference 5. The isolated nacelle was shown in figure 10, and its F-function was shown in figure 11. Since the nacelles were mounted symmetrically on the configuration, the F-functions of each pair were calculated by doubling the magnitude of the F-function in figure 11. This "nacelle-pair" F-function was transferred to the appropriate effective-length stations on the conceptual aircraft F-function axis and added with it.

## Nacelle-Wing Interference Lift

The equivalent areas due to the incremental nacelle-wing interference lift produced by each pair of nacelles was computed using the method described in reference 5. From these equivalent areas, figure 12, the F-function, figure 13, from the nacelle-wing interference lift equivalent areas of each nacelle pair were calculated with the *ARAP* code, reference 8.

## F-Function Summation And Pressure Signature Calculation.

The F-function from the conceptual aircraft's volume (without nacelles), the wing lift, the canard lift, and canard-wing interference lift, figure 9, were added to the F-function from the nacelle volume, figure 11, and the F-function of the nacelle-wing interference lift, figure 13, to provide a complete conceptual aircraft F-function, shown with solid line, in figure 14. The dashed line in figure 14 showed sections of the F-function from figure 9 which did not include nacelle-volume and nacelle-wing interference lift effects.

All four nacelles were located well aft of the concept's nose, and the F-functions from the nacelle volume effects and the nacelle-wing interference lift effects were added at the station where their effects began. The discontinuities at the beginning of the nacelle volume and the nacelle-wing interference lift F-functions were given special treatment. Discontinuities seen at 170 and 175 feet were due to the nacelle-pair volumes, while the discontinuity at 185 feet was caused by the nacelle-wing interference lift. In this analysis, F-function values were combined at 5-foot intervals, so the initial F-function had to be recalculated so that the first and the second F-function values preserved the initial impulse under the nacelle-wing interference lift F-function. Since the ground-level pressure signature was desired, no significant error was introduced by the treatment given to this F-function.

This combined F-function represented the sonic-boom disturbance potential of the entire canard-wing conceptual aircraft at the beginning-cruise altitude, Mach number, and weight. It could now be used as input data to the *ARAP* disturbance-propagation code so that the ground-level pressure signature beneath the flight path, solid-line pressure signature in figure 15, could be calculated. The comparison pressure signature in figure 15, designated by the dashed line, was calculated from the F-function in figure 9, which had no nacelle volume or nacelle-wing interference lift effects.

# Results

Aircraft geometry and cruise requirements were used to analyze the sonic-boom characteristics of a conceptual canard/wing high-speed civil transport. Equivalent area distributions from the volume and the lift were calculated so that Whitham F-functions could be computed and summed to obtain an F-function describing the disturbance potential of the whole concept. Finally, the ground-level pressure signatures were predicted from this summed F-function, and interpreted with the aid of the generated equivalent areas and component F-functions.

Both predicted pressure signatures were regarded as N-waves since the mini-shock on the nacelles-off signature would be smoothed over by its passage through the real atmosphere. The nacelles had increased the positive impulse (area under the positive part of the overpressure curve) by about 16 percent, the strength of the nose shock by 0.22 psf, and the strength of the tail shock by 0.20 psf. So the noise experienced indoors, which depends mainly on the impulse, might be slightly more annoying. However, the noise heard outdoors was determined almost entirely by the magnitude of the overpressure, and would be about the same from either of the pressure signatures if they propagated through a standard stratified atmosphere.

The effect of the canard was easy to see on the area distribution in figure 8 and the F-functions in figures 9 and 14. However, it did not appear as a significant factor in the nacelles-off pressure signature (dashed line) in figure 15. The mini-shock on this signature was contributed by wing lift seen as the pronounced "camel-hump" on the F-function in figure 9, and to a lesser degree from the slope change near the peak of the area distribution in figure 8. Since the effects of the wing lift, the nacelle volume, and interference-lift were dominant factors in generating the nose shock strength, the lifting canard did not significantly alleviate the sonic boom of this configuration.

To be of significant value as a low-boom feature, the canard would have to be moved forward closer to the nose. In this more forward location, it's downwash effects would be somewhat reduced, though not eliminated. Moreover, it's lift would be a little more effective as a rotation-inducing force during takeoff and low-speed flight. As a result, it might be possible to reduce the configuration's size and weight.

While the results of this analysis seemed to indicate the canard was not very effective as a reduced-boom lifting surface on this configuration, they did not indicate that a lifting canard would be of little or no value *on all configurations*. The results of this paper demonstrated that special analytic treatment had to be given to a concept where both a canard and a wing provided lift during cruise. At the same time, the analysis should be considered an indication that more design and analysis work would be required before the use of a lifting canard could be considered as mission-useful on this, or any, low-boom concept.

# Concluding Remarks

A method for analyzing the sonic-boom characteristics of a canard/wing aircraft when both the wing and the canard surfaces were carrying lift has been presented, discussed, and demonstrated. The design and analysis methods developed during the 1980s were modified to specify that a configuration F-function would be calculated from two types of F-functions. Smooth-and-continuous equivalent areas would be used to obtain the first set of F-functions. A second set of F-functions would be calculated when the normal or equivalent areas were from components like ducted nacelles, nacelle-wing interference lift, or lifting surfaces with long sections of supersonic leading edge. These smooth-area and non-smooth-area F-functions would then be summed to obtain a concept F-function for predicting a ground overpressure signature. Since the canard was a special addition to the usual simple wing/fuselage/nacelle/fin configuration, a canard-wing performance analysis code was employed to provide estimates of force and pitching moment coefficients for cruise-mission performance analysis, and the equivalent area distributions of canard-wing interference lift for sonic-boom prediction calculations.

An example of a conceptual canard-wing configuration, with lift provided by both the canard and the wing during cruise, was used to demonstrate the application of the method. Two ground-level overpressure signatures were calculated and discussed. The first pressure signature was from volume and lift contributions that were mathematically smooth and continuous, while the second signature included nacelle volume and nacelle-wing interference lift contributions which had discontinuities caused by the ducted engine nacelle geometry. Both of the predicted ground-level pressure signatures were N-wave in shape with similar nose- and tail-shock strengths. It was concluded, from the shapes of the F-functions and the pressure signatures, that the small differences in nose and tail shock strengths were due mainly to the location of the engine nacelles. A lift-carrying canard surface did not seem to be of help in the reduction of the ground-level sonic boom from this conceptual aircraft. However, no general conclusions could be made about the potential benefits of a lifting canard on a low-boom-tailored conceptual aircraft design because the required component integration and low-boom tailoring tasks had not been performed.

No cruise range, takeoff field length, balanced field length, or rudder-power calculations were performed because the emphasis was placed on obtaining a prediction of the overpressure when the vehicle employed a lifting canard, and on ascertaining the increments in sonic-boom performance when a lifting canard was employed to lengthen the lift distribution. It was noted, however, that a canard generating lift during cruise did cause a drag increment and a corresponding lift/drag ratio decrement due to the wing's location in the canard's downwash field. If the wing and canard can be positioned so that this drag penalty can be aerodynamically minimized, then there might be sonic-boom benefits to be realized.

# References

1. Mack, Robert J.; and Needleman, Kathy E.: *A Methodology For Designing Aircraft To Low Sonic Boom Constraints*. NASA TM-4246, 1991.

2. Mack, Robert J.: *Some Considerations On The Integration Of Engine Nacelles Into Low-Boom Aircraft Concepts*. High-Speed Research: Sonic Boom, Volume II, NASA Conference Publication 3173, 1992.

3. Craidon, Charlotte B.: Description Of A Digital Computer Program For Airplane Configuration Plots. NASA TM X-2074, 1970.

4. Harris, Roy V., Jr.: *A Numerical Technique For Analysis Of Wave Drag At Lifting Conditions*. NASA TN D-3586,1966.

5. Mack, Robert J.: *A Numerical Method for Evaluation and Utilization Of Supersonic Nacelle- Wing Interference*. NASA TN D-5057, 1969.

6. Carlson, Harry W.; and Mack, Robert J.: *Estimation Of Wing Nonlinear Aerodynamic Characteristics at Supersonic Speeds*. NASA TP-1718, 1980.

7. Shrout, Barrett L.: *Extension Of A Numerical Solution For The Aerodynamic Characteristics Of A Wing To Include A Canard Or Horizontal Tail*. Paper presented at AGARD Specialists Meeting on Aerodynamic Interference (Silver Springs, MD.), September 1970.

8. Hayes, Wallace D.; Haefeli, Rudolph C.; and Kulsrud, H. E.: *Sonic-Boom Propagation In A Stratified Atmosphere, With Computer Program*. NASA CR-1299, 1969.

9. Whitham, G. B.: *The Flow Pattern Of A Supersonic Projectile*. Communication on Pure and Applied Mathematics, vol. V, no. 3, August 1952, pp. 301 - 348.

10. Walkden, F.: *The Shock Pattern of a Wing-Body Combination, Far From The Flight Path*. Aeronautical Quarterly, vol. IX, pt. 2, May 1958, pp. 164 - 194.

**Appendix A. Summary of physical and mission characteristics of the HSCT-14 concept.**

<div align="center">Concept Description</div>

| | |
|---|---|
| Span, ft | 132.0 |
| Length, ft | 310.0 |
| Wing reference area, $ft^2$ | 10,483.5 |
| Wing aspect ratio | 1.66 |
| Canard span, ft | 40.0 |
| Canard projected area, $ft^2$ | 498.4 |
| Canard control surface area, $ft^2$ | 309.0 |
| Canard aspect ratio | 3.21 |
| Fin area, $ft^2$ | 488.0 |
| Number of engines | 4 |
| Thrust per engine, lb th | 55,000 |

<div align="center">Mission Data</div>

| | |
|---|---|
| Mission range, nmi | 5000.0 |
| Number of passengers | 300 |
| Cruise Mach number | 2.4 |
| Beginning-cruise altitude, ft | 56,400 |
| Cruise $C_L$ | 0.09139 |
| End-cruise altitude | 66,200 |

<div align="center">Mission Weights (preliminary estimates)</div>

| | |
|---|---|
| Gross take-off weight, lb | 770,000 |
| Empty weight, lb | 316,000 |
| Beginning-cruise weight, lb | 693,000 |
| End-cruise weight, lb | 434,000 |
| Fuel weight, lb | 389,000 |
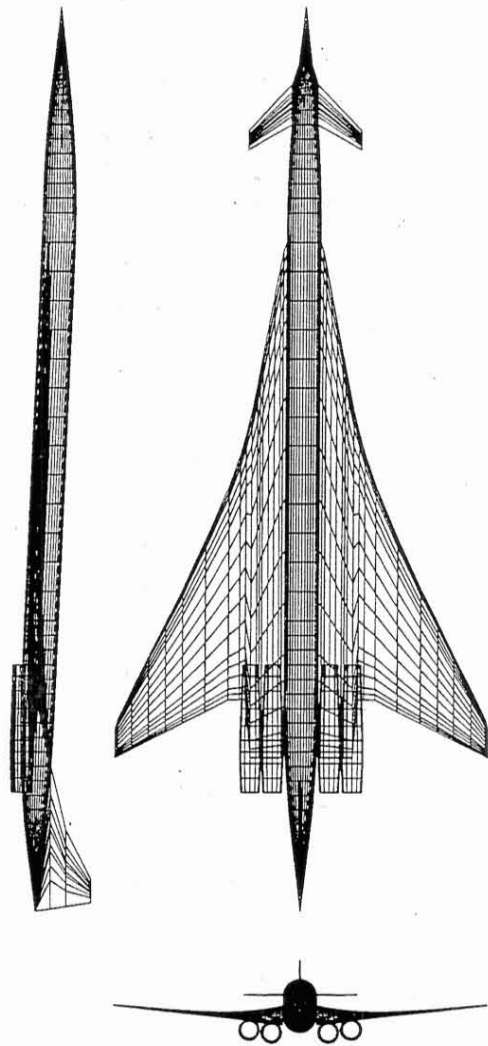
Figure 1. Three-view sketch of the HSCT-14 conceptual aircraft.
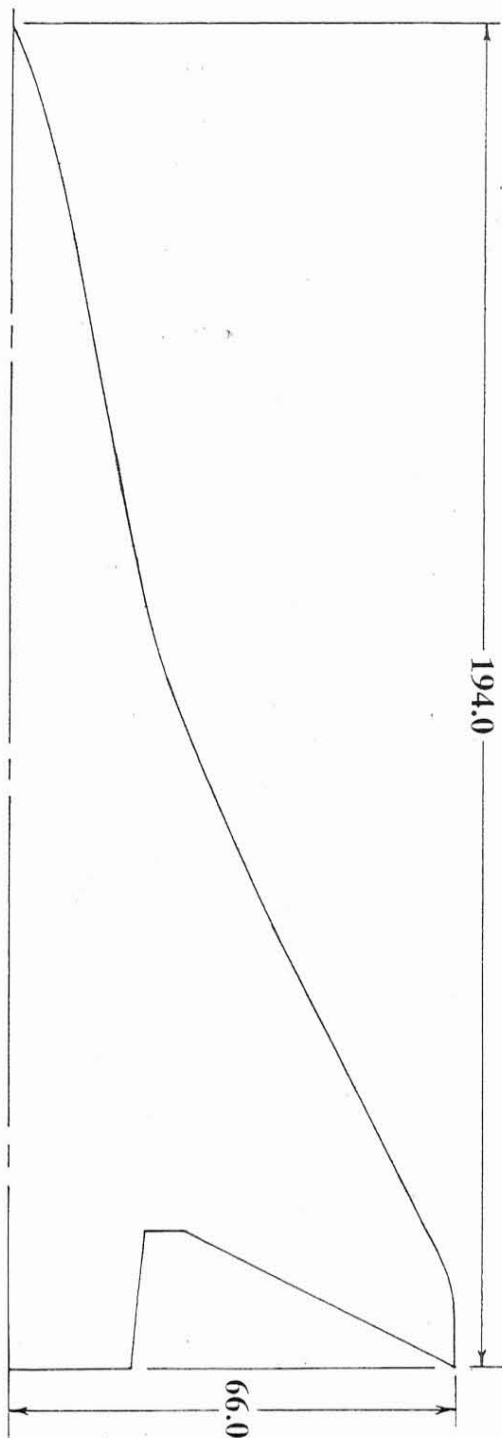
Figure 2. HSCT-14 wing planform.

194.0

66.0
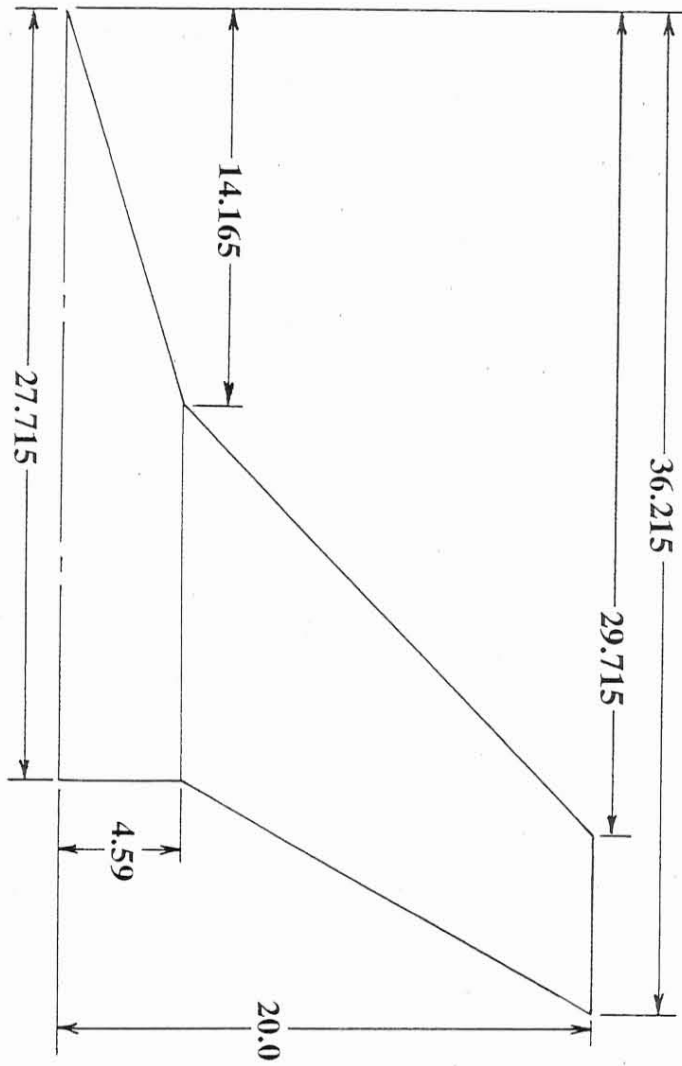
Figure 3. HSCT-14 canard planform.
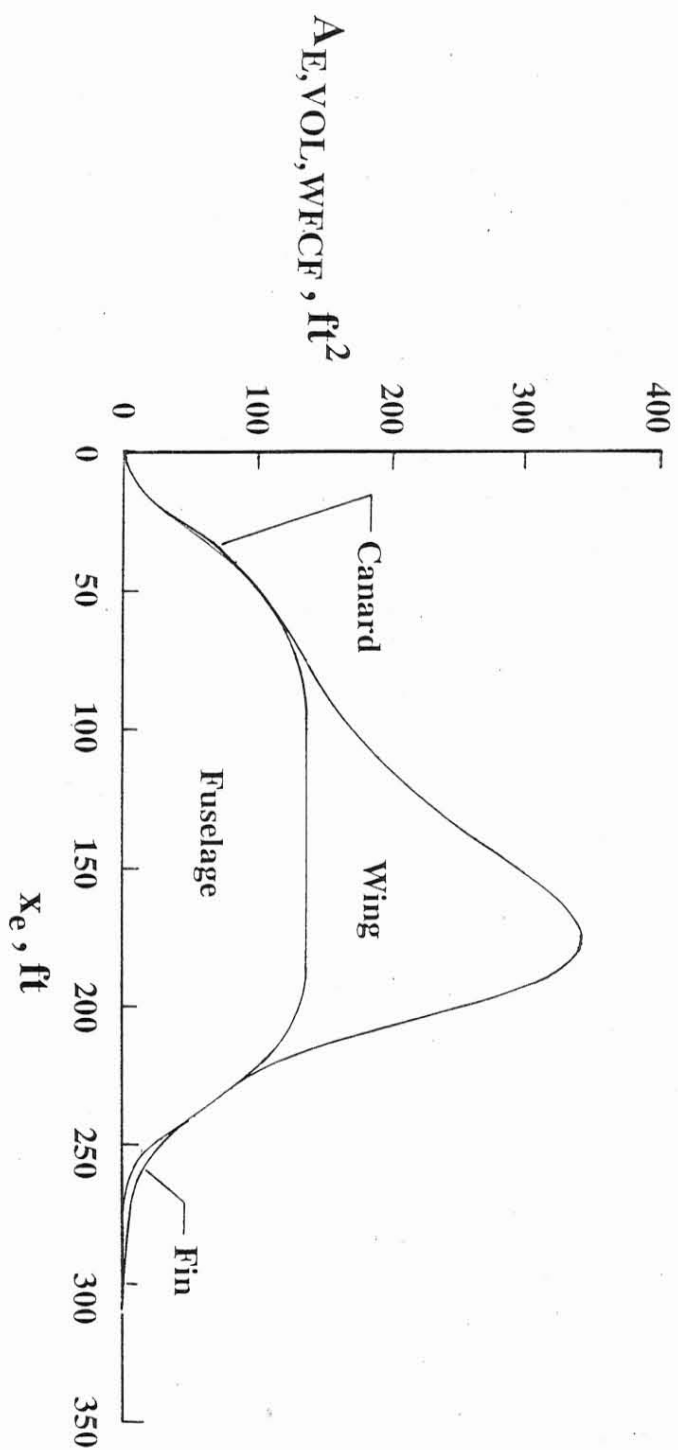
Figure 4. Equivalent areas due to volume of the wing, fuselage, canard, and fin.
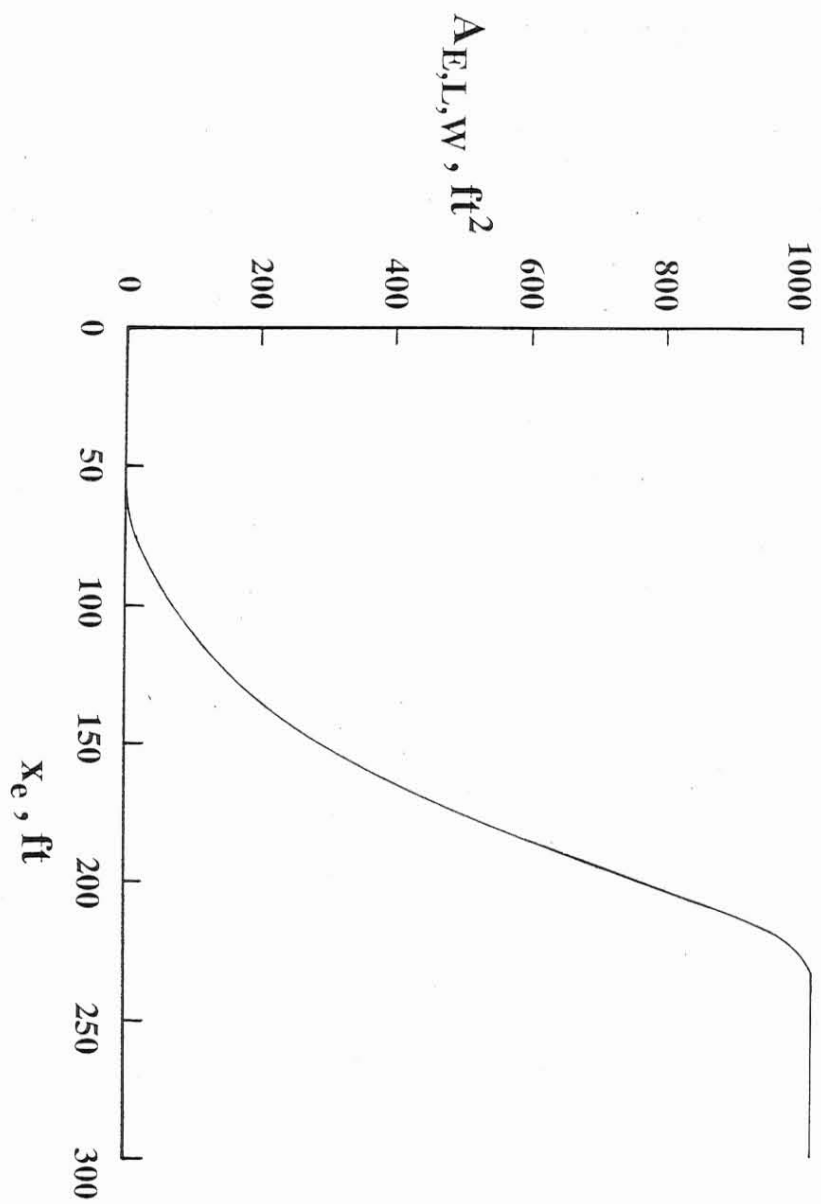
Figure 5. Equivalent area due to isolated wing lift.
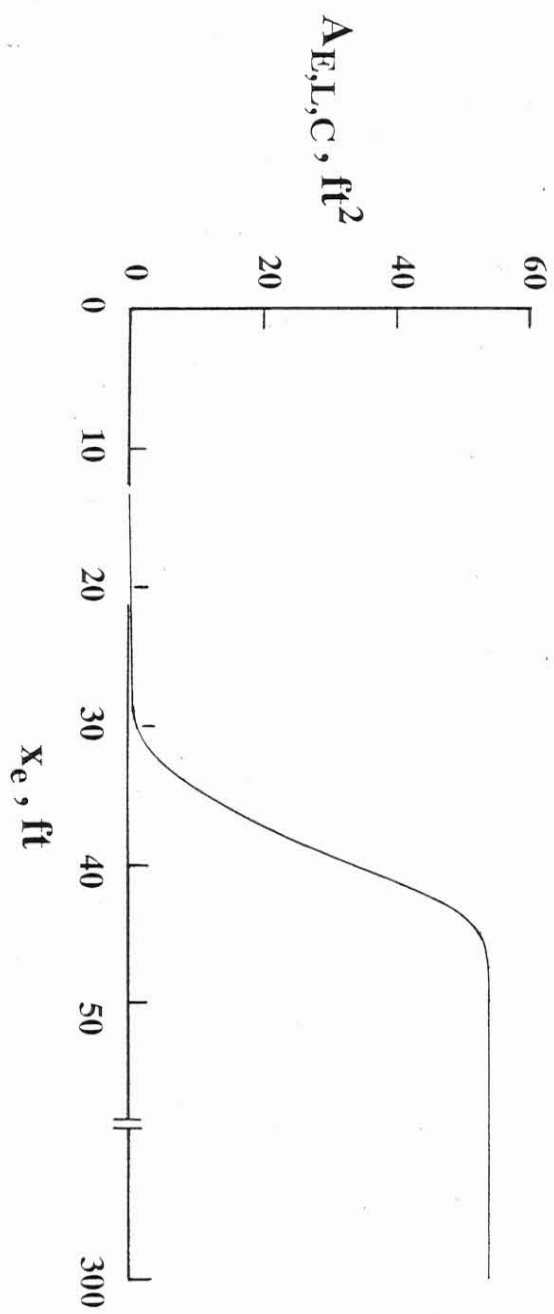
Figure 6. Equivalent area due to isolated canard lift.
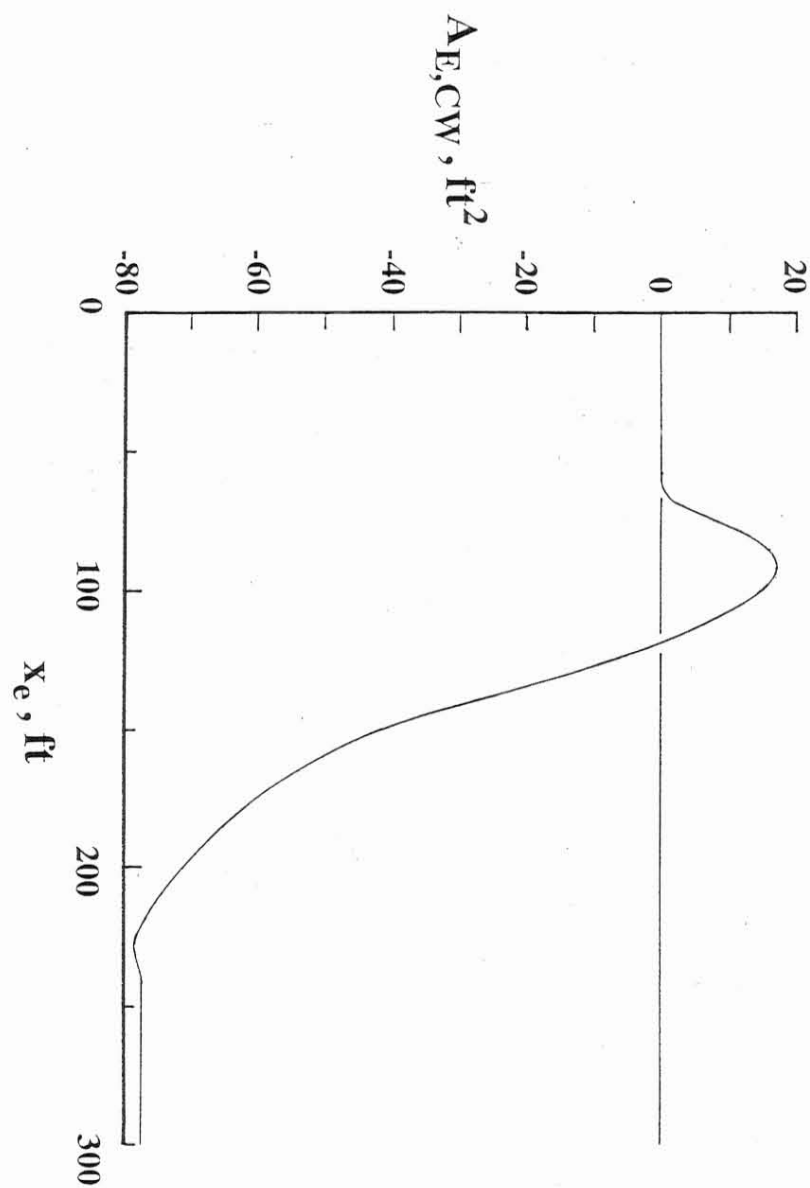
Figure 7. Equivalent area due to canard-wing interference lift.

24
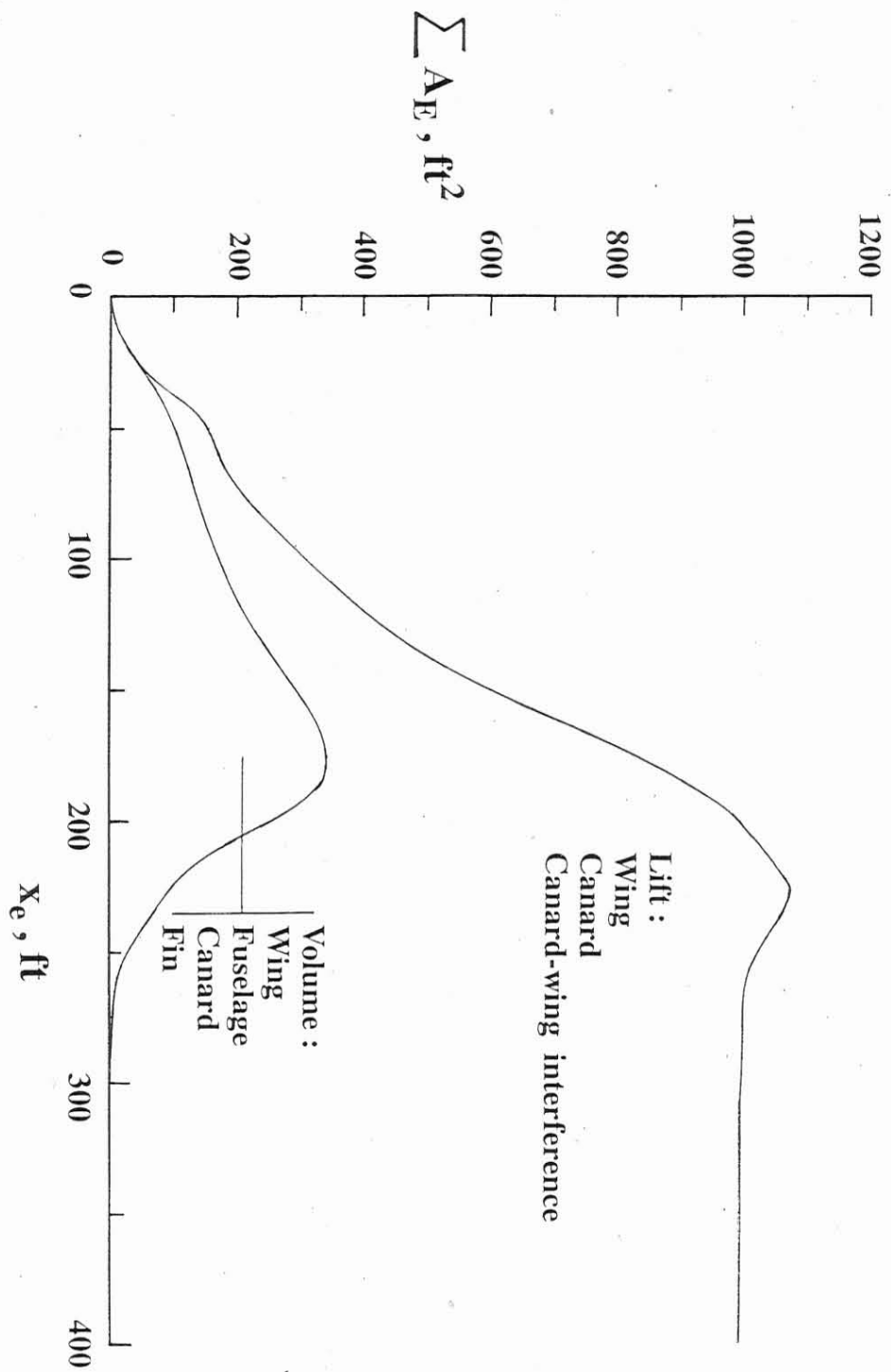
Figure 8. Sum of equivalent area due to volume and lift without nacelle effects.

$\sum A_E, ft^2$

$x_e, ft$

Lift :
Wing
Canard
Canard-wing interference

Volume :
Wing
Fuselage
Canard
Fin
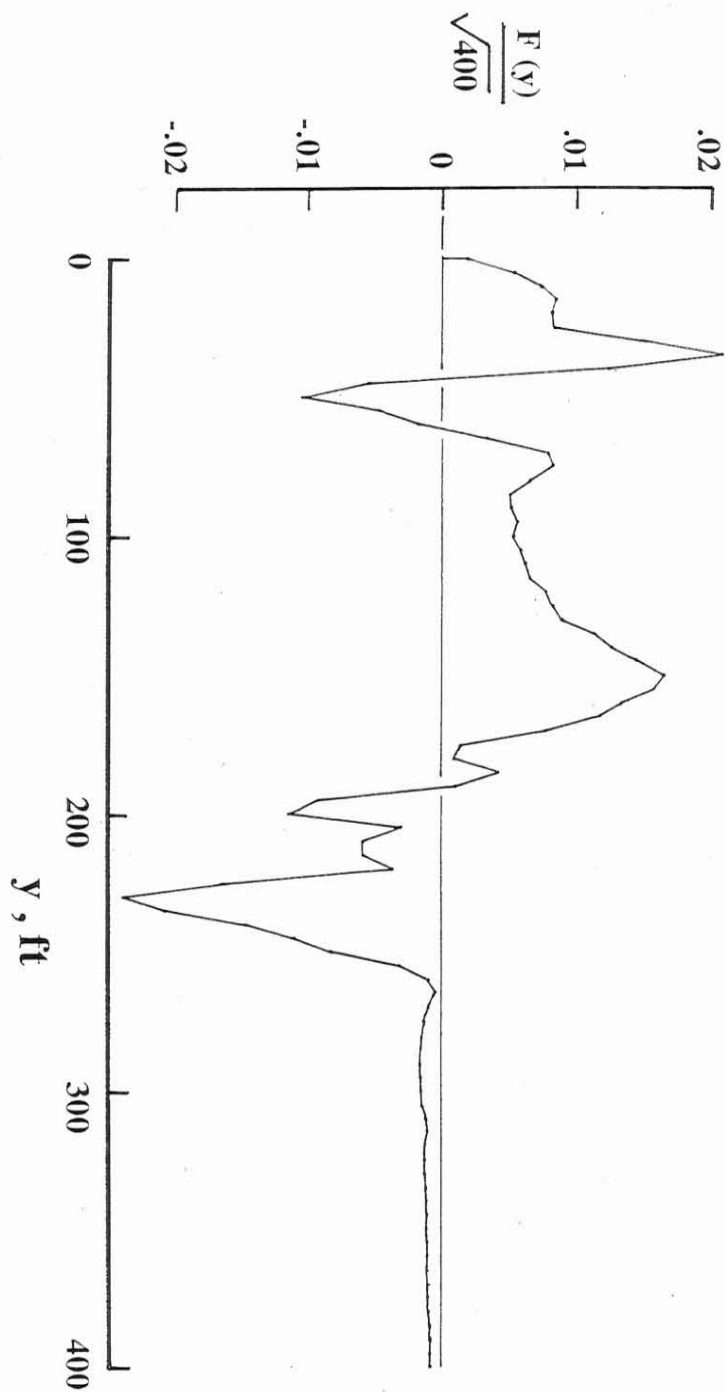
Figure 9. F-function of the HSCT-14 volume and lift without nacelle effects.

26
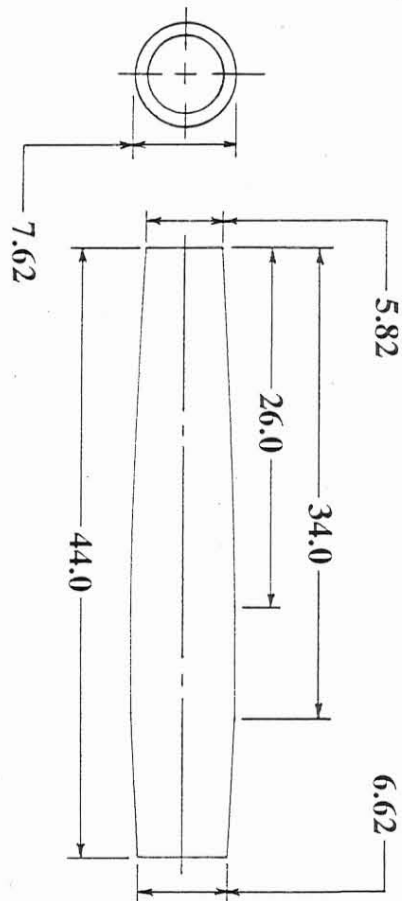
Figure 10. Two-view sketch of a HSCT-14 engine nacelle.
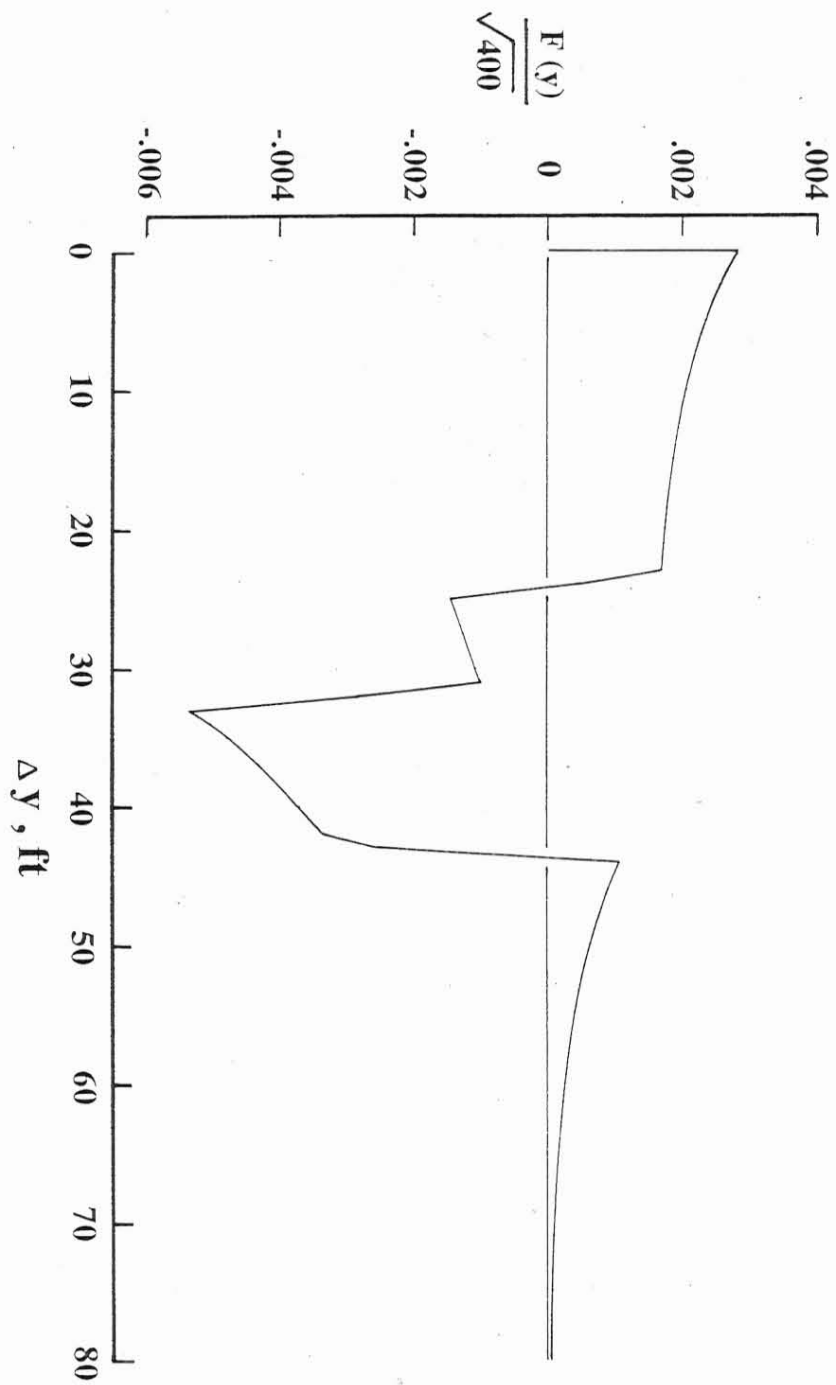
Figure 11. F-function of a HSCT-14 engine nacelle.
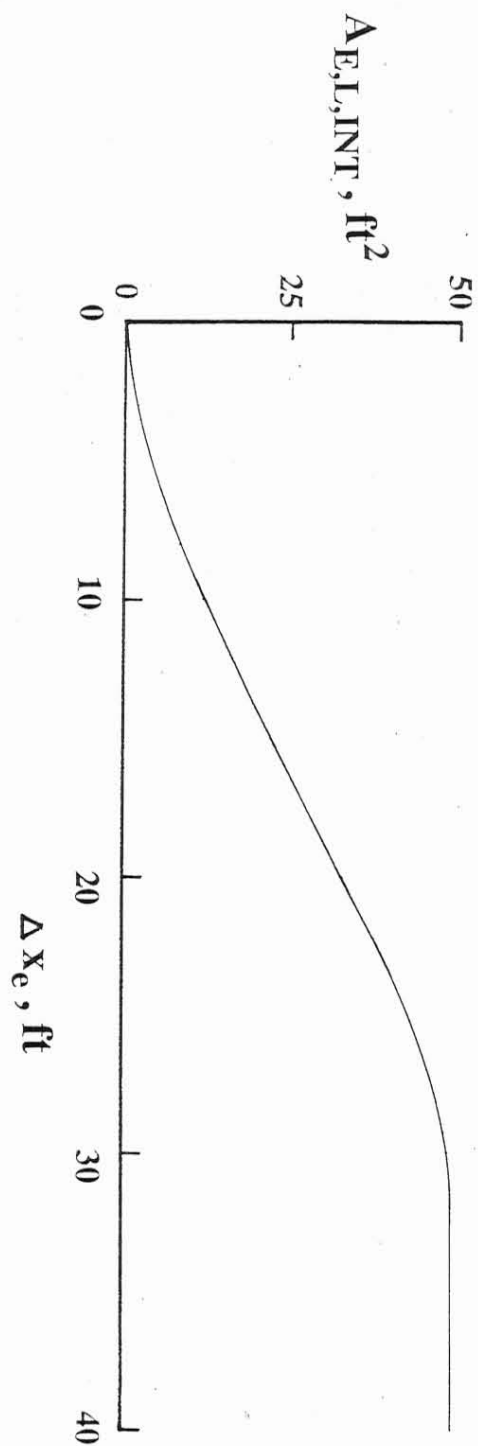
Figure 12. Total equivalent area due to nacelle-wing interference lift.
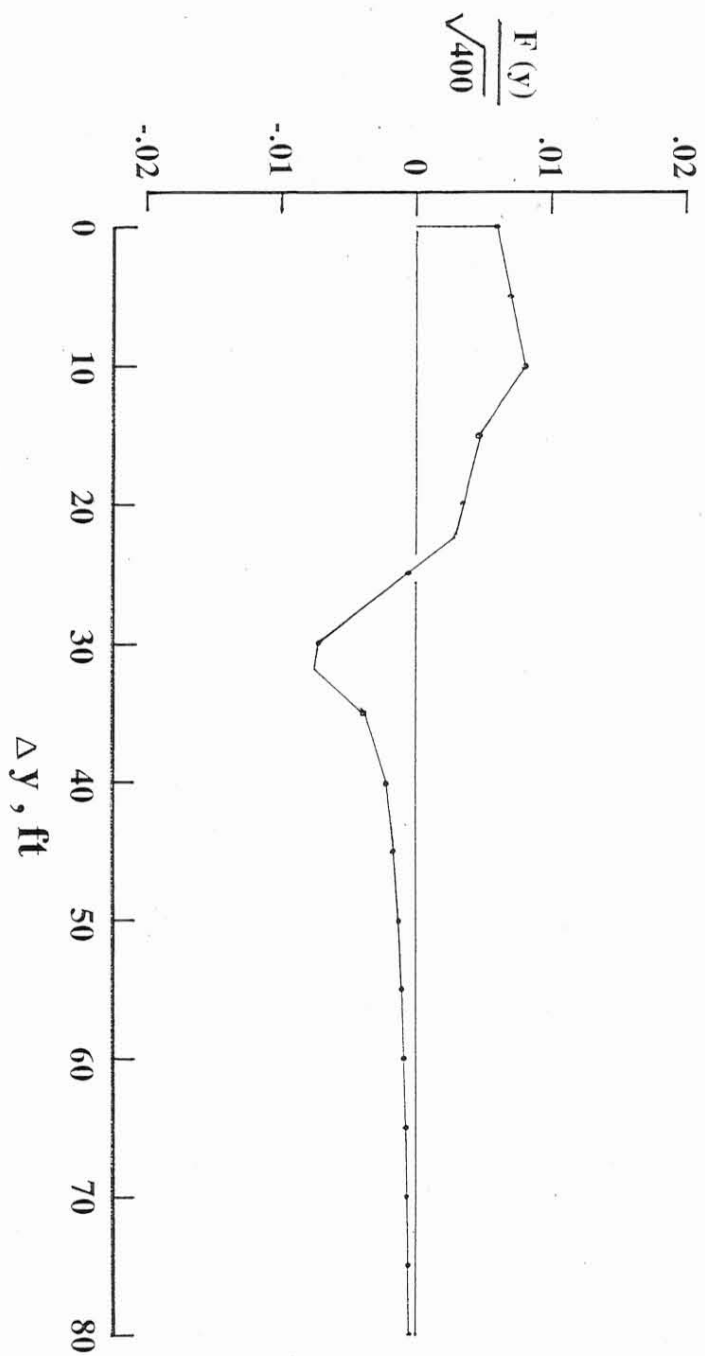
Figure 13. F-function of the total nacelle-wing interference lift.
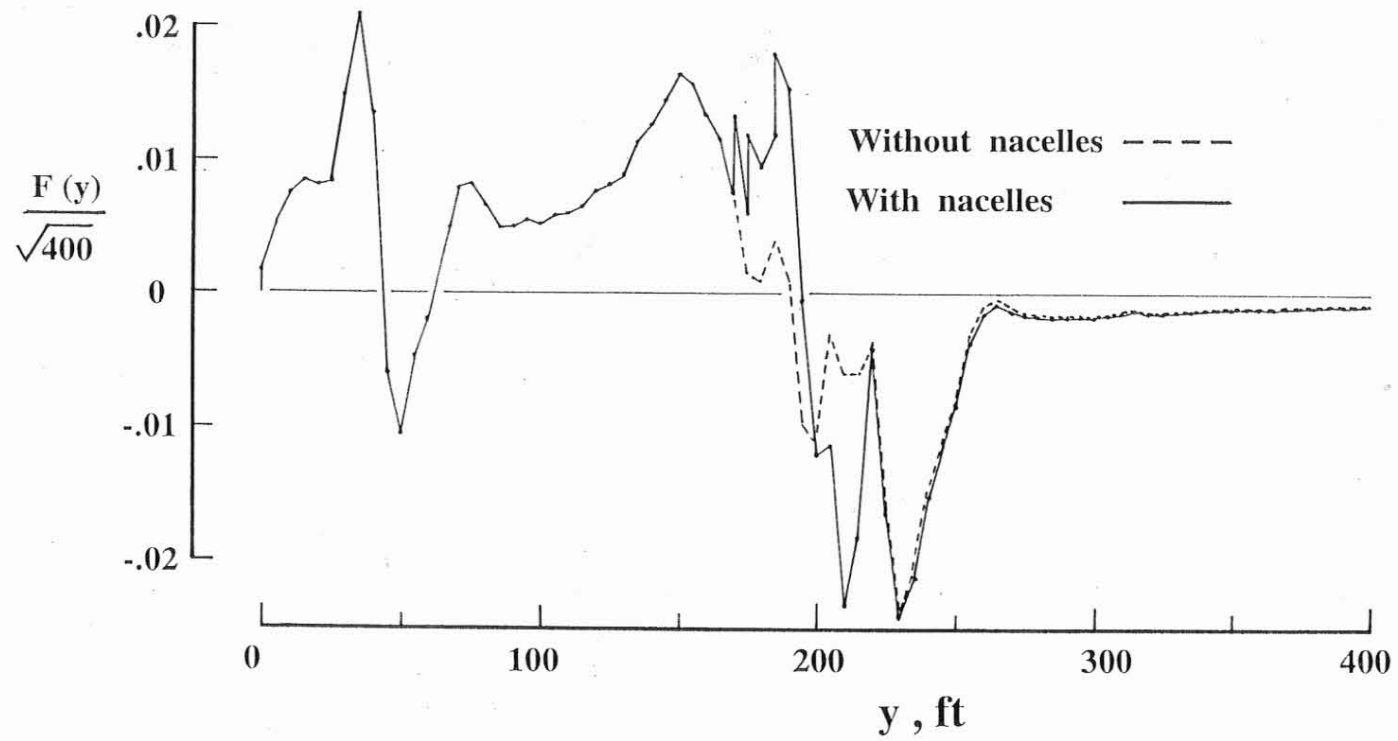
Figure 14. F-function of the HSCT-14 volume and lift including nacelle effects.
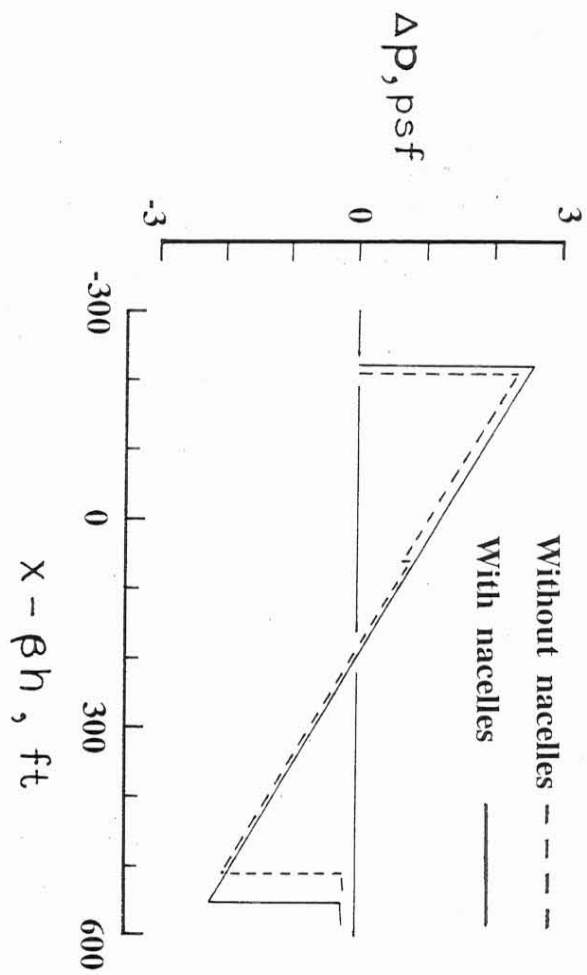
Figure 15. Ground-level predicted pressure signatures at M = 2.40, h = 56,400 ft, and $W_{CR}$ = 693,000 lb.

# REPORT DOCUMENTATION PAGE

| 1. REPORT DATE *(DD-MM-YYYY)* | 2. REPORT TYPE | 3. DATES COVERED *(From - To)* |
|---|---|---|
| 01- 12 - 2005 | Technical Memorandum | |

**4. TITLE AND SUBTITLE**

Method for Estimating the Sonic-Boom Characteristics of Lifting Canard-Wing Aircraft Concepts

**5a. CONTRACT NUMBER**

**5b. GRANT NUMBER**

**5c. PROGRAM ELEMENT NUMBER**

**6. AUTHOR(S)**

Mack, Robert J.

**5d. PROJECT NUMBER**

**5e. TASK NUMBER**

**5f. WORK UNIT NUMBER**

984754.02.07.07

**7. PERFORMING ORGANIZATION NAME(S) AND ADDRESS(ES)**

NASA Langley Research Center
Hampton, VA 23681-2199

**8. PERFORMING ORGANIZATION REPORT NUMBER**

L-19176

**9. SPONSORING/MONITORING AGENCY NAME(S) AND ADDRESS(ES)**

National Aeronautics and Space Administration
Washington, DC 20546-0001

**10. SPONSOR/MONITOR'S ACRONYM(S)**

NASA

**11. SPONSOR/MONITOR'S REPORT NUMBER(S)**

NASA/TM-2005-213930

**12. DISTRIBUTION/AVAILABILITY STATEMENT**

Unclassified - Unlimited
Subject Category 71
Availability: NASA CASI (301) 621-0390

**13. SUPPLEMENTARY NOTES**

An electronic version can be found at http://ntrs.nasa.gov

**14. ABSTRACT**

A method for estimating the sonic-boom characteristics of a conceptual aircraft at supersonic cruise where the lift is carried by both a canard and the wing is presented, discussed, and demonstrated. The method employed several updated wing, canard, canard-wing interference, and sonic-boom analysis codes to evaluate the concept's mission performance and predict its sonic-boom ground overpressures. A hypothetical lifting-canard 1 wing concept was designed and used as an example to demonstrate the method.

**15. SUBJECT TERMS**

Whitham theory; Sonic boom; Canard-wing concept

| 16. SECURITY CLASSIFICATION OF: | | | 17. LIMITATION OF ABSTRACT | 18. NUMBER OF PAGES | 19a. NAME OF RESPONSIBLE PERSON |
|---|---|---|---|---|---|
| a. REPORT | b. ABSTRACT | c. THIS PAGE | | | STI Help Desk (email: help@sti.nasa.gov) |
| U | U | U | UU | 37 | 19b. TELEPHONE NUMBER *(Include area code)* (301) 621-0390 |